


Natural image noise removal using non local means and hidden Markov models in stationary wavelet transform domain

Asem Khmag¹  · Syed Abdul Rahman Al Haddad² ·
Ridza Azri Ramlee² · Noraziahtulhidayu Kamarudin² ·
Fahad Layth Malallah³

Received: 28 March 2017 / Revised: 2 November 2017 / Accepted: 14 November 2017 /
Published online: 1 December 2017
© Springer Science+Business Media, LLC, part of Springer Nature 2017

Abstract In self-similarity digital image features, nonlocal means (NLM) exploits the major aspects when it comes to noise removal methods. Despite the high performance characteristics that NLM has proven, computational complexity yet to be highly achieved especially in case of complicated texture patches. In this regard, this study uses the clustered batches of noisy images and hidden Markov models (HMMs) in order to achieve noiseless images where the dependency between additive noise model pixels and its neighbors on stationary wavelet transform is found using HMMs. This paper is helpful and significant in order to develop a speedy and efficient plant recognition system computer-based to identify the plant species. The pivotal significant of the use of NLM and HMMs in this study is to ensure the statistical properties of the wavelet transform such as multiscale dependency among the wavelet coefficients, local correlation in neighbourhood coefficients. Practically, the experimental

✉ Asem Khmag
khmaj2002@gmail.com

Syed Abdul Rahman Al Haddad
sar@upm.my

Ridza Azri Ramlee
ridza@utem.edu.my

Noraziahtulhidayu Kamarudin
hidayu.kamarudin@gmail.com

Fahad Layth Malallah
Fahad.layth.86@gmail.com

¹ Faculty of Engineering, Zawia University, Zawia, Libya

² Faculty of Engineering, Universiti Putra Malaysia, Serdang, Malaysia

³ Faculty of Computer Science, Cihan University, Sulaimani, Iraq

results present that the proposed algorithm has depicts high visual quality images in the experiments that are conducted in this study, apart from the objective analysis of the proposed algorithm, the execution time and its complexity show a competitive performance with state of the art noise removal methods in low and high noise levels.

Keywords Additive noise · Non-local means · Hidden Markov model · Spatial filter · Image denoising · Multiscale clustering

1 Introduction

Several noise removal techniques work in either spatial domain or frequency domain [25]. Spatial denoising methods have the advantages of simple algorithm structure and high image quality in low noise levels. However, their performances decayed in sever noise models and complex textures of tested images especially the digital images with repeated patterns [7]. From theoretical point of view, most of transform domain methods does not show an adequate results particularly in real-time applications due to the loopholes in hardware limitation and manufacturing issues.

In this regard, NLM filters [2] utilizes the original characteristics which are mostly appear in the repeated textures of the digital images and then shows an output images which have very clear details both in its presence and visual quality. The pivotal difference between NLM and the bilateral and spatial domain filters is that NLM exploits merits of statistical structures that represented by mean and local correlation in the contaminated patches, instead of using only a few samples in specific area of the noisy images like what local filters do [26]. In addition, recent studies highlighted on the way of increasing speed of NLM technique in terms of its calculation processes such as matching and searching procedures due to the long consuming time that NLM is taken. As a result, many techniques are developed to eliminate the different patches before weighted averaging process carries out. In recent study by [13], the visual quality of a natural digital image deteriorates by the noise model of impulse type during the record or transmission situation. Their experimental results concluded that the proposed technique can efficiently remove salt-and-pepper noise from noisy images for several noise levels and the denoised image is freed from the blurred and Gibbs phenomenon. Another study by [17] combined adaptive vector median filter (VMF) and weighted mean filter in order to remove high-density impulse noise from colored digital images. They found that their method outperformed (~1.5 to 6.2 dB improvement) some of the recent techniques not only at low noise levels but at high-density impulse noise as well. On the same regard, Chen and Qian in [3] have reached to an algorithm that suppressed the noise from hyperspectral digital images where they utilized stationary wavelet approach principle component analysis to reduce the dimensionalities. Despite the high quality noise removal results, execution time of this method was the real burden. Support vector machine (SVM) was exploited in study that represented by [5]. An empirical model has been created in order to remove the noise from hyperspectral images. Yet to get rid of the cost in the time execution which is their technique showed. In order to improve the boundary discriminative noise detection, filter that proposed in [6] was used and uncorrupted pixels are calculated within the processing window in order to scan the while entire noisy image. A novel adaptive iterative fuzzy filter for denoising images corrupted by impulse noise was proposed by [1]. They used two stages-detection approach for noisy pixels with an adaptive fuzzy detector and then applied denoising processes using a weighted

mean filter. Experimental results demonstrated high image quality compared to best standard image denoising techniques where it showed robustness performance even in high noise levels. A switching median filter is proposed to be applied on a fuzzy-set framework. Schulte et al. in [16] proposed two-stage nonlinear noise removal method worked according to fuzzy logic procedure. Whereas multiclass SVM based adaptive filter (MSVMAF) has been introduced for removal of multiplicative noise from RGB images. Furthermore, PCA shows its high performance when it comes to the reduction dimensionality issues. On the other hand, over-complete approach which utilizes shift spinning technique was used in this study in order to enhance the denoised image quality especially in high noise levels and sharp edges in the image textures and other delicate parts [9, 10] where in [10] there was no any NLM filters or any classification approaches to classify the corrupted pixels from the noise free ones.

In study that was proposed by Li et al. in [12], an image block-based noise detection rectification method was introduced in order to estimate the contaminated density of a tested image. The experimental results have depicted that their technique could dramatically improve the denoising and blur effects. Moreover, another study proposed by in [11] it utilized the local statistics for additive white Gaussian noise in order to estimate additive Gaussian noise. In their study, the approach included selecting low-rank sub-image with removing high-frequency components from the contaminated image. The results were efficiently outperformed state of the art noise estimation methods in a wide range of visual contents and noise conditions. In MRI image type, Nayak et al. presented an automatic classification system for segregating pathological brain from normal brains in magnetic resonance imaging scanning [15]. In the same regard, Zhang et al. utilized SWT in order to extract the features instead of DWT, their experimental results on a normal brain MRI demonstrate that wavelet coefficients via SWT is superior compared to the traditional wavelet transformation DWT [27].

In the current study, an algorithm based on the NLM procedure and utilize the coefficient correlation in different levels is proposed. In addition, to minimize the interference of the AWGN in the preclassification step, stationary wavelet semi-soft thresholding approach is firstly utilized in classification of the contaminated patches. Afterward, the HMM filter is adopted to capture the dependencies among the coefficients in the transform domain, as well as smooth the image and reduce the noise prior to thresholding. The experimental results show that this method outperforms several up-to-date denoising methods in terms of both peak signal-to-noise ratio (PSNR) and image appearance. The paper contains number of contributions. Firstly, it presents an HMM-based invariant similarity quantity to catch the dependency of contaminated coefficients with AWGN and increase the number of candidates for nonlocal mean filtering. The other contribution is that the suggested algorithm shows a high performance in comparison with ordinary NLM and up-to-date denoising methods at several noise levels.

2 Related work

In terms of the original NLM method and its updated filters, the main idea of NLM is according to the fact that sub-images in a whole image mostly contain a self-similarity pixels, where the image patches share the same structure and textures as line squares and geometric shapes [21]. Given a contaminated image, the resulted intensity of the investigated pixel

$NL(u)(i)$ computed as a weighted average of the whole intensity amount within the same location I . [2]:

$$NL(u)(i) = \sum_{j \in I} w(i, j) u(j) \quad (1)$$

$u(j)$ being the pixel intensity at the location j , and $w(i, j)$ being the weight of $u(j)$ in order to measure the connection among the investigated pixels i and j , L is the number of elements in each cluster. The specific weights are computed using the following expression.

$$w(i; j) = \frac{1}{z(i)} \exp^{-\frac{\|u(N_i) - u(N_j)\|_{2,a}^2}{h^2}} \quad (2)$$

N_i is the patch with stationary size and it is located at pixel i . In this case, the similarity can be calculated as a shrinking model that utilizes the weighted Euclidean distance. The case where $a > 0$ is known by the standard deviation of the kernel of Gaussian function, and $Z(i)$ is a constant and represents the normalization amount where $Z(i) = \sum_j w(i, j)$, and

h represents the parameter function of the filter.

In order to find the set of consistent candidates which are similar to the patch under testing from a complete digital image, three main classes of techniques are used, Preclassification step, and to find the updated similarity groups and finally to apply applying HMMs to catch the dependencies among similar patches.

Preclassification process was previously utilized to deal with only the part of the patch searching rather than the full testing of the whole image in order to attain high efficiency of NLM. However, most of modified versions of NLM contribute only in few margins of improvements when it comes to noise removal results. In [14], a study exploited the mean quantity and local average gradient vectors as well in order to ignore unrelated sub-images. On the other hand, the criterion might only be used when the gradient magnitudes of the main patches are lasted in a value of threshold more than the desired amount, which can be very easy to be adjusted by additive white Gaussian noise. A preclassification approach based on sub-image variance was similarly proposed in [4].

The main disadvantage of the earlier mentioned techniques is that their entire structure is very complicated, despite it is not built according to any statistical models, such as correlation among coefficients in the same neighborhood. In [20], SVD was implemented in order to utilize some statistical properties to keep its gradient structure to be used in k-means clustering. Consequently, the gradient structure of the image shows a sever sensitivity to the noise level amount. Additionally, there is one more loophole in the traditional NLM; this disadvantage is that there are no enough candidates for each patch to be used in weighted averaging when an image lacks repetitive patterns. This deficiency will radically show its impact on the visual appearance of the images that resulted from NLM.

In order to conquer this effect, a study in [8, 23] developed a rotated matching technique that utilize the block procedure to achieve more similar sub-images, though the scheme is basically restricted to specific number of rotation angles and images with simple textures. Finding out updated similarity methods is another manner to guarantee reliable group of candidates using wavelet transforms.

In [19], block matching based on moment invariants were introduced, which is invariant under rotation processes, blurring, and noise. In order to attain the main objective of finding further reliable groups of candidates, the proposed technique utilizes both preclassification and

definition of the updated similarity model. However, the chance of finding candidates for non-repetitive patterns [20] is needed to be implemented. Therefore, preclassification step is exploited to provide suitable candidate sets which can be built from the whole parts of the tested image. In addition, in [25] a method utilized clustering according to NLM using invariants of specific moments to be as classification step was introduced. Furthermore, they have adopted a technique that uses the rotationally of each block matching in sub-images in order to increase the matching rate. High PSNR values and good image quality have been achieved but their method was time consuming due to matching processes. Markov models can also be considered in each state corresponding to a deterministically observable experience. Hidden Markov models (HMMs) are essentially first-order discrete time series with some hidden information. In other words, the time series states are not the observed information but are connected through an abstraction to the observation. Consequently, the result of such sources in any given state is not random. This model is somehow considered a restrictive technique that is applicable to many problems of interest [10]. As a result, the notion of Markov models should be extended to contain the case in which the reflection is a probabilistic model of the state. That is, the resulting concept (called an HMM) is a doubly embedded stochastic procedure with a fundamental stochastic process, which is not observed directly. On the contrary, the process is observed only throughout the stochastic process of another set that yields the structure of observations. Specifically, the state sequence is one whose states are not uniquely determined according to the observation of sequence of the output and the knowledge of the original state [7].

Defining a new similarity term that can evaluate the noisy coefficients and suppress the noise in the contaminated image is thus essential.

3 NLM based on stationary wavelet transformation and HMMs

The pipeline processing of the proposed technique is shown in Fig. 1. Given a contaminated image, the main aim is to result a noise removal image in which the noise is eliminated and most of the fine structures are reserved. The image is corrupted by additive noise $n_{i,j}$ and one observes the noisy image as $y_{i,j}$, such that:

$$y_{i,j} = x_{i,j} + n_{i,j} \quad (3)$$

Similar to (1) and (2), the suggested NLM can be expressed as follows:

$$NL(u)(i) = \sum_{j \in \mathcal{I}} w_R(i,j) u(j) \quad (4)$$

$$w_R(i,j) = \frac{1}{Z_R(i)} \exp\left(-\frac{d_R(i,j)}{h^2}\right) \quad (5)$$

v is the noisy image, $w_R(i,j)$ is depended on the updated distance quantity $d_R(i,j)$ and $Z_R = \sum_j w_R(i,j)$. The weighted averaging is accomplished in each bunch. In addition, L reflects the number of components in every cluster. The impact of clustering is shown

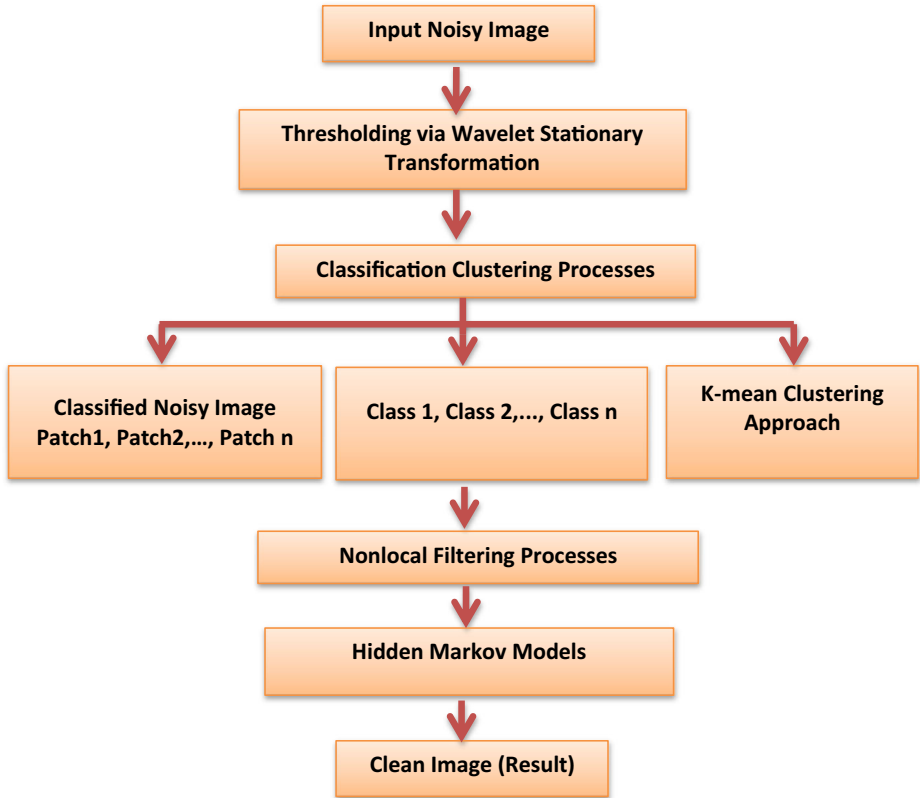


Fig. 1 Block diagram of the proposed natural image denoising algorithm

in Fig. 2. Furthermore, the filtering issue thus changes into how the updated weights $[w_R(i, j)]$ can be calculated, which is elaborated in coming Subsections.

The proposed NLM has the following features:

- Filtering process using semi-soft thresholding in stationary wavelet domain provides the pre-processing for preclassification. The main impact is depicted in Fig. 2.



Fig. 2 (a) Noisy image with Gaussian noise $\sigma = 25$. (b) Filtered image with semi-soft thresholding

- Clustering of K-means on moment invariants of the distorted contaminated image assists as a preclassification model for the proposed noise removal technique. In the traditional NLM, most investigated sub-images have a stable size of candidate groups which either take the entire signal or the only a sub-group of neighborhood which is located at selected patch.
- HMM on the wavelet domain is the main step to design the proposed algorithm. The relationship between noise-free image, AWGN, and corrupted image can be represented by (5).

3.1 Preprocessing stage

In this step, the main classification process is applied basically on the structural information of the tested image. Thus, patch-based preclassification in a contaminated image will show inaccurate evaluation [23]. As a result, a pre-filter approach will be considered to smooth the image and thus avoid dealing with the incorrect patches, especially in severe noise cases.

In practice, estimating the standard deviation σ of the noise is an essential task in the proposed algorithm, and it should be performed from the image rather than assumed as given. The noise level can be estimated empirically from the finest scale HH_1 . Moreover, the coefficients of stationary wavelet transform are stated as a correlated group of data and are linked with few patches in the same neighborhood. The large wavelet coefficients mostly will reflect large coefficients in the same neighborhood. As a result, the suggested thresholding is found up from the coefficients that last in the same investigated zone of the contaminated image. In this regard, presume $B_{i,j}$ is wavelet coefficient that lies in the target noisy image. Then:

$$U^2_{i,j} = \frac{B^2_{i,j-1} + B^2_{i,j} + B^2_{i,j+1}}{3} \quad (6)$$

In the Equation, $U^2_{i,j}$ represents the summation of the square of the terms which is centered at the same side of the coefficient under the thresholding process, while (i,j) shows the coefficients which lie in the contaminated image. The following situation is considered if:

$$U^2_{i,j} \geq \lambda^2 \quad (7)$$

3.2 Clustering procedure

In several fields, moment invariants are utilized, such as skin detection, image registration, image deblurring, and shape recognition, to name a few. Previous studies showed that it is robust to be used as image descriptors under different applications such as shifting, changing in its value, and applying spin processes. In [19], the moments that have greater invariants were shown their performance to be more susceptible when the noise of Gaussian mode takes place. As a result, in the proposed technique that exploits Hu's moment invariants [19], which have peak order of 2, are used as feature descriptors with size of (1×5) vector for the clustering of K-means. In this regard, consider a $N \times N$ size of digital whole-image and a $n \times n$ sub-image that is located at i ($i = 1, 2, \dots, N \times N$), the moment-invariants of the sub-group is presented by

the vector of size of 1×5 . As a result, regarding to the entire image; the tested image with size of $N \times N$ vectors that works as the initial signal of the clustering of K-means.

Then the tested coefficients $B_{i,j}$ substituted by zero; else, it will be shrunk based on the following formula:

$$\hat{B}_{i,j} = \frac{B^2_{i,j} - \lambda^2 B^2_{i,j}}{U^2_{i,j}} \tag{8}$$

$$\lambda = \sqrt{2 \ln M_j} \times \sigma_w, \tag{9}$$

where σ_w is the standard deviation of the corrupted image, and M_j depicts the size of coefficients in a sub-band under investigation at the analysis edge j . Equation (10) summarizes the semi-soft thresholding approach.

$$\hat{B}_{i,j} = T(B_{i,j}, \lambda) = \begin{cases} 0 & U^2_{i,j} \geq \lambda^2 \\ \frac{B^2_{i,j} - \lambda^2 B^2_{i,j}}{U^2_{i,j}} & U^2_{i,j} < \lambda^2 \end{cases} \tag{10}$$

After the semi-soft thresholding is utilized on the contaminated image, the hazy image assists as the contribution of grouping. This input is demonstrated clearly in Fig. 2.

$$\arg \min_c = \sum_{k=1}^K H(Gb(i)) \in Hm_k \sum_{i=1,2,\dots,N \times N} (|H(Gb(i)) - \mu_k|^2) \tag{11}$$

In the above mentioned equation, $Gb(i)$ denotes the Gaussian blurred sub-image which is located at i . $H(\cdot)$ represents the output the moment invariants of an input sub-image. In addition, μ_k is considered as the mean vector for the k^{th} cluster $Hm_k \dots$. Afterwards, K clusters $Hm_1, Hm_2, Hm_k, \dots, Hm_K$ can be achieved. Every single cluster Hm_k is composed of L vectors and Hm_{kl} ($k = 1, \dots, K, l = 1, 2, \dots, L$). In the same issue, the high efficient technique which adopts an iterative refinement procedure is utilized [21]. Furthermore, clustering technique which utilizes K-means offers the pre-selected candidates for the selected weighted averaging. The resulted data of the desired classification (the matches of the center of sub-image) is located at form of a look-up table. Weighted averaging structure is performed inside every single cluster throughout the next step.

3.3 HMMs-based Non-local mean method

In this step, the parameters of the HMM template can be obtained in each block using $\prod_{k,d} = \{p_{s_{k,d}}(m), \sigma^2_{k,d,m}\}$, where p is the number of states in the independent mixture model, and the label in the each position i can be represented by D_i . In denoising-based wavelet transform, the aim is to minimize the MSE between the estimated and the original image. This step can be done by calculating the minimizing MSE between the estimated wavelet coefficients of the denoised and the original image. As a result, the image denoising process can be considered as process of estimating wavelet coefficients of the original image from coefficients of the wavelet signal of the noise and the contaminated image. Given that the distribution of each coefficient in the wavelet realm of the noisy image W_i

is stated as a Gaussian mixture model (GMM), and the probability density function PDF of W_i is given by

$$f_{W_{i,k}}(w_{i,k}) = \sum_{m=1}^2 P_{S_{k,d}}(m) f_{W_{i,k}|S_{k,d}}(w_{i,k}|S_{k,d} = m) \quad (12)$$

In terms of the relationship among the specific coefficients of the noise, the relationship of the noisy image and the original image is as follows:

$$x_{i,k} + n_{i,k} \quad (13)$$

where $w_{i,k}$, $x_{i,k}$, and $n_{i,k}$ refer to the wavelet coefficients of the contaminated input image, the image, and the noise; $n_{i,k}$ is AWGN; and *iid* with variance σ_n^2 . Thus, the distribution of the original image $x_{i,k}$ is GMM as well, and if the value of the hidden state S_k is determined, then the estimation issue can be considered as estimating a Gaussian signal in the AWGN in order to reduce the MSE. The following Eq. (14) is used to achieve the Gaussian estimation:

$$E[X_{i,k}|W_{i,k}, S_k = m] = \frac{\sigma_{k,m}^2}{\sigma_{k,m}^2 + \sigma_n^2} w_{i,k} \quad (14)$$

$X_{i,k}$ and $W_{i,k}$ are random variables of $x_{i,k}$ and $w_{i,k}$ respectively, P_{S_k} is the probability mass function (PMF) of the hidden state $S_{i,k}$, and $\sigma_{k,m}^2$ is the variance of the component $X_{i,k}$.

Therefore, by applying the transition criteria and adding the hidden states to Eq. (14), the estimation criteria become

$$E[X_{i,k}|W_{i,k}] = \sum_{m=1}^2 P_{S_k}(m) \frac{\sigma_{k,m}^2}{\sigma_{k,m}^2 + \sigma_n^2} w_{i,k} \quad (15)$$

The independent mixture model is used to join the PDF of the coefficients in the wavelet domain at the same block. Hence, Eq. (15) is utilized to evaluate and estimate the coefficients of the noise-free image in the block under study. With the block label stated, the formula can be modified as

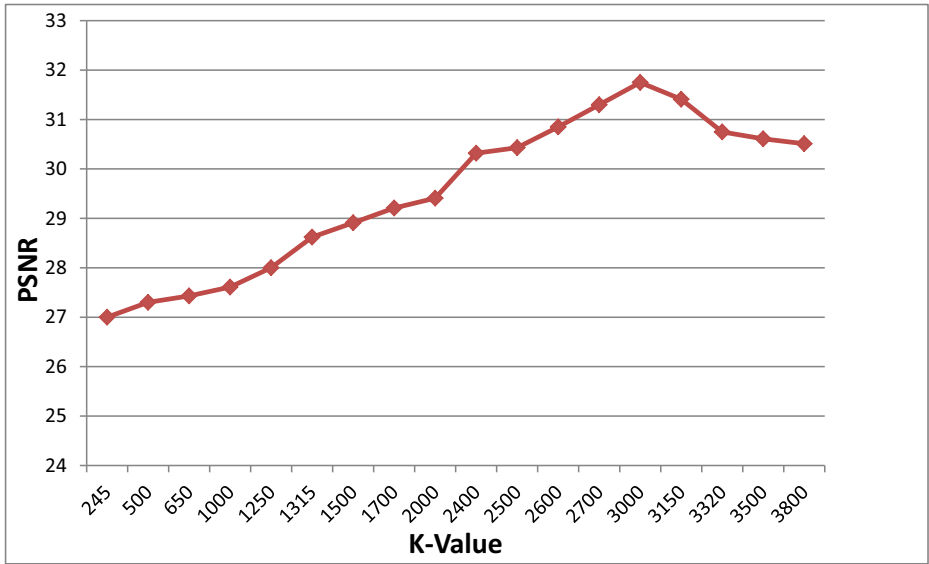
$$E[X_{i,k}|W_{i,k}, D_{i,k} = d] = \sum_{m=1}^2 P_{S_k}(m) \frac{\sigma_{k,m}^2}{\sigma_{k,m}^2 + \sigma_n^2} w_{i,k} \quad (16)$$

where $X_{i,k}$, $D_{i,k}$, and $W_{i,k}$ are the random variables of $x_{i,k}$, the block label, and $w_{i,k}$, respectively; and P_{S_k} is the PMF of the hidden states $S_{i,k}$, whose block label is d . In addition, $\sigma_{k,m}^2$ is considered as the variance of the component $X_{i,k}$, which has the same block label d .

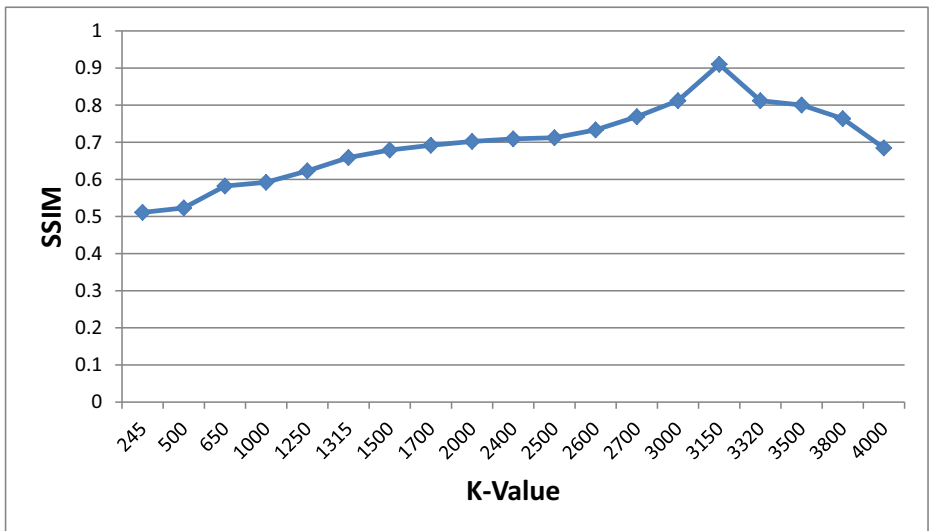
As the variance of $X_{i,k}$ cannot be derived directly from the estimation, the denoised image variance can be obtained from the noisy image, and then the redundant variance resulted from the noise can be subtracted.

4 Experimental results

In the experiment part, the images used in the experimental purposes are all standard grayscale and natural testing images. The benchmark tested images are selected from a popular image database, the USC-SIPI Database Images (University of Southern California). For performance evaluation, the proposed method will be compared to the conventional NLM and the recent



(a) PSNR average values



(b) SSIM average values

Fig. 3 PSNR and SSIM values fluctuate with K in noise level $\sigma = 20$

related techniques [8, 24] according to the specific dataset. The evaluation metrics adopted in the experiments are structural similarity index (SSIM) and peak signal to noise ratio (PSNR). PSNR is exploited in order to provide objective evaluations of the noise removal image results. It is expressed by the following formula:



Fig. 4 Performances of the clustering analysis of the proposed technique when K is 256

$$PSNR = 10 \cdot \log_{10} \left(\frac{MAX^2}{MSE} \right) \tag{17}$$

As eq. (17) shows, MAX is representing the dynamic size of the tested image, MSE is the mean squared error between the tested and the noise removal images. For instance, if the noisy image contains 8 bits per pixel, it can be formed with a pixel scale range of 0 to 255. A higher PSNR value shows higher-quality image and noise reduction results. On the other hand, SSIM [22] is a metric that has a kind of consistency with human visual perception. Regarding to this, SSIM is expressed by [8]:

$$SSIM(x, y) = [I(x, y)]^\alpha [c(x, y)]^\beta [s(x, y)]^\gamma \tag{18}$$

Note that $\alpha > 0$, $\beta > 0$, and $\gamma > 0$, whose parameters are used to arrange the modules.

$$I(x, y) = \frac{2\mu_x\mu_y + c_1}{2\mu_x^2 + 2\mu_y^2 + c_1} \tag{19}$$

$$c(x, y) = \frac{2\sigma_x\sigma_y + c_2}{2\sigma_x^2 + 2\sigma_y^2 + c_2} \tag{20}$$

$$s(x, y) = \frac{\sigma_{xy} + c_3}{\sigma_x\sigma_y + c_3} \tag{21}$$

where $\mu_x = \sum_{i=1}^N w_i x_i$, μ_x represents the mean of the original image; $\sigma_x = \left(\sum_{i=1}^N w_i (x_i - \mu_x) \right)^{\frac{1}{2}}$; σ_x represents the standard deviation of the original image; $\sigma_{xy} = \sum_{i=1}^N w_i (x_i - \mu_x) (y_i - \mu_y)$; σ_{xy} represents the cross standard deviation through the tested image and the noisy one; w represents the circular symmetric Gaussian weighting function; and C_1 , C_2 , and C_3 are the three constants to prevent instability.

4.1 Parameters of clustering

The proposed clustering method is implemented based on moment invariants. Several parameters need to be decided for standard K-means clustering, such as type of distance used,

Table 1 Average PSNR of different noise removal techniques

Image	Technique	$\sigma = 10$	$\sigma = 20$	$\sigma = 35$	$\sigma = 45$	$\sigma = 55$	$\sigma = 70$
Man	NLM	30.6096	28.9415	24.0274	22.1212	19.8203	13.1412
	Sven et al. [19]	31.9042	28.9987	24.1578	22.4784	20.6564	13.5502
	Yan et al. [25]	31.8033	30.1200	25.7073	22.7810	23.1468	13.8011
	Khmag et al. [9]	31.8242	28.8611	24.8500	22.3438	20.4130	13.3263
	Proposed	32.0102	30.8102	26.6174	23.6332	24.7196	14.2148
Monarch	NLM	31.7868	30.1013	28.2138	26.3589	24.5918	20.1412
	Sven et al. [19]	31.8556	30.1111	28.2655	26.0098	25.0907	22.3415
	Yan et al. [25]	32.8840	30.9815	29.2523	27.2328	26.3026	24.9040
	Khmag et al. [9]	31.8723	30.1089	28.2201	26.3509	24.8309	21.2420
	Proposed	33.4125	31.6274	30.2210	27.8586	27.012	25.7101
Lena	NLM	30.1205	28.7988	27.2832	25.6843	24.1319	19.8145
	Sven et al. [19]	30.7659	28.8802	27.3558	26.0087	24.6223	21.0876
	Yan et al. [25]	31.3885	30.0122	28.4804	26.9449	26.1124	23.7858
	Khmag et al. [9]	30.6501	28.8401	27.2939	25.8191	24.3247	20.9642
	Proposed	32.1120	29.8472	28.9002	27.1591	26.7101	24.8301
House	NLM	32.1434	30.0025	27.9899	26.0446	24.3105	19.8429
	Sven et al. [19]	32.3352	30.8816	28.0953	26.5455	25.9618	22.3722
	Yan et al. [25]	33.4783	31.1976	29.0268	28.0454	26.9828	25.8292
	Khmag et al. [9]	32.2691	30.6283	28.0632	26.8232	25.3170	21.1021
	Proposed	33.8874	31.9001	29.7423	28.9157	27.4021	26.5550
Peppers	NLM	31.4137	29.5473	27.6721	25.8659	24.1645	19.7590
	Sven et al. [19]	32.0053	30.5619	27.8097	26.6315	24.4551	21.0076
	Yan et al. [25]	33.6801	31.1678	29.0657	27.4582	26.2204	23.6793
	Khmag et al. [9]	32.0061	30.1267	27.7028	25.9801	24.2798	20.0069
	Proposed	33.9031	31.6601	29.7102	27.8888	26.7531	24.0002
Boat	NLM	30.8749	29.1526	27.3969	25.7290	24.0721	19.8365
	Sven et al. [19]	31.1523	30.0052	27.4430	25.8831	24.4548	21.1243
	Yan et al. [25]	33.2810	30.7653	28.5930	27.0240	26.0495	24.2728
	Khmag et al. [9]	31.0902	29.4396	27.4411	25.7333	24.2223	20.4229
	Proposed	33.8114	31.9012	29.1121	28.5544	26.8740	24.7986
Baboon	NLM	32.4352	30.5207	28.4973	26.4933	24.7115	20.1715
	Sven et al. [19]	32.5744	30.6654	28.9895	26.0971	25.0092	22.5567
	Yan et al. [25]	33.0517	31.2918	30.0415	28.9240	27.6842	26.6160
	Khmag et al. [9]	32.5440	30.6372	28.6192	26.3137	24.9922	21.4375
	Proposed	33.7140	31.4442	30.8100	29.3363	28.0012	27.1010
F-16	NLM	30.3578	28.8968	27.1939	25.7950	24.1379	19.9039
	Sven et al. [19]	31.1236	29.6548	28.2336	26.6559	25.8819	22.0012
	Yan et al. [25]	31.9462	31.0414	30.3732	27.6452	27.1293	23.5498
	Khmag et al. [9]	31.0952	29.3622	27.7197	25.8648	24.6300	21.0938
	Proposed	32.7744	31.4910	30.8021	28.7713	27.8088	24.0021
Straw	NLM	33.5255	31.3356	29.0487	26.8699	24.9479	20.1644
	Sven et al. [19]	33.6413	32.0187	29.1559	27.0901	25.9089	22.7390
	Yan et al. [25]	33.8645	31.8396	29.8417	28.6245	27.6680	25.3085
	Khmag et al. [9]	33.5893	31.9411	29.3689	26.9885	25.2123	21.1424
	Proposed	34.0021	32.3939	30.4003	29.0012	28.1411	25.9099

quantity of clusters assigned, and length of vector parameters utilized in the suggested NLM-based framework. In practice, the Euclidean distance is exploited to measure the distance between two significant feature vectors as [14] showed. Based on study in [18], the sub-image size chosen is 7×7 . In order to examine how the effect of the technique fluctuates with several values of K , we tuned K in the range of 350 and 4200. The results of PSNR and SSIM of the

Table 2 Average PSNR and SSIM values of different techniques

σ	NLM		Sven et al. [19]		Yan et al. [25]		Khmag et al. [9]		Proposed	
	PSNR	SSIM	PSNR	SSIM	PSNR	SSIM	PSNR	SSIM	PSNR	SSIM
10	31.49	0.8508	31.97	0.8572	32.81	0.8918	31.87	0.8562	33.88	0.9334
20	29.70	0.7811	30.09	0.7948	30.94	0.8424	30.07	0.7871	31.74	0.9101
35	27.84	0.6983	28.05	0.7243	29.18	0.7694	28.05	0.6992	30.82	0.8753
45	26.05	0.6144	26.26	0.6733	27.62	0.7035	26.21	0.6200	28.24	0.7412
55	24.34	0.5360	25.06	0.5963	26.65	0.6630	25.05	0.5493	27.19	0.6881
70	19.94	0.3947	21.77	0.4731	24.57	0.5741	21.28	0.4020	26.01	0.6520

investigated images (noise level σ is 20) with different cluster numbers are depicted in Fig. 3. The main fluctuating trends of both scales PSNR and SSIM are mostly compatible. By other words, when K increases, the number of current clusters which are represented from different types of image fine structure increases as well. Thus, in the case where K becomes particularly high, then there will not be enough clusters candidates. Consequently, the measured PSNR and SSIM decrease next to the climax. Furthermore, if the complexity of the algorithm is not the main target, the optimal amount of K can be chosen according to the input size of the

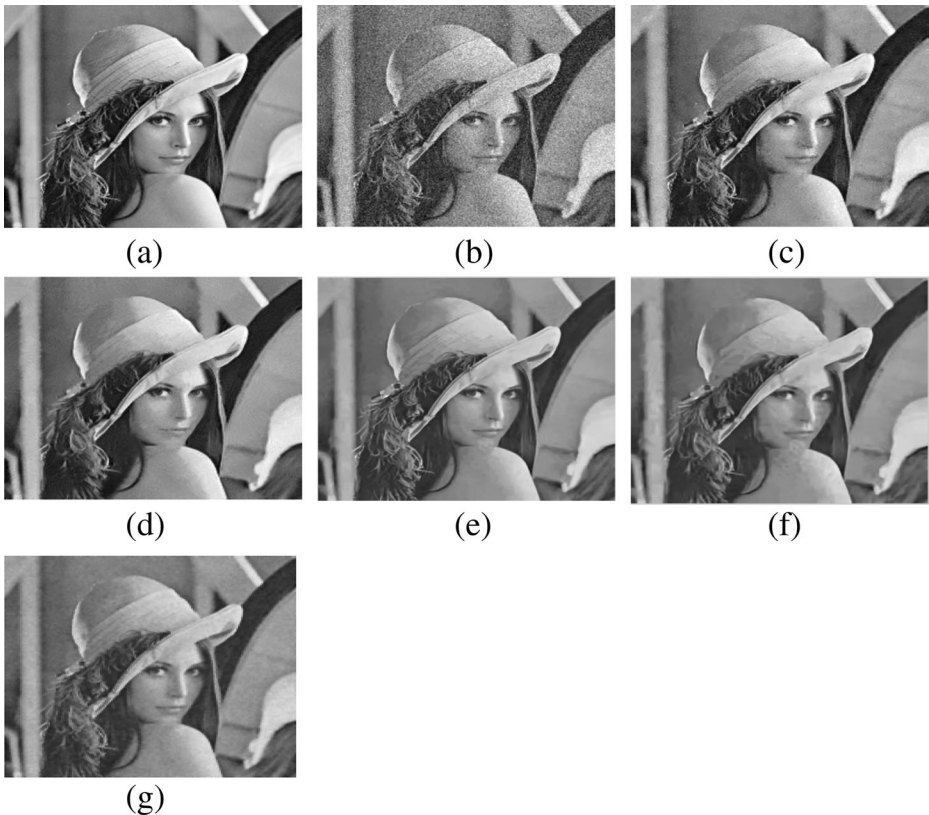


Fig. 5 Comparison of different denoising methods visual results when noise level is 20 for benchmark image Lena. (a) Noise-free image, (b) Noisy image, (c) NLM, (d) Sven et al. [19], (e) Proposed algorithm, (f) Yan et al. [25], (g) Khmag et al. [9]

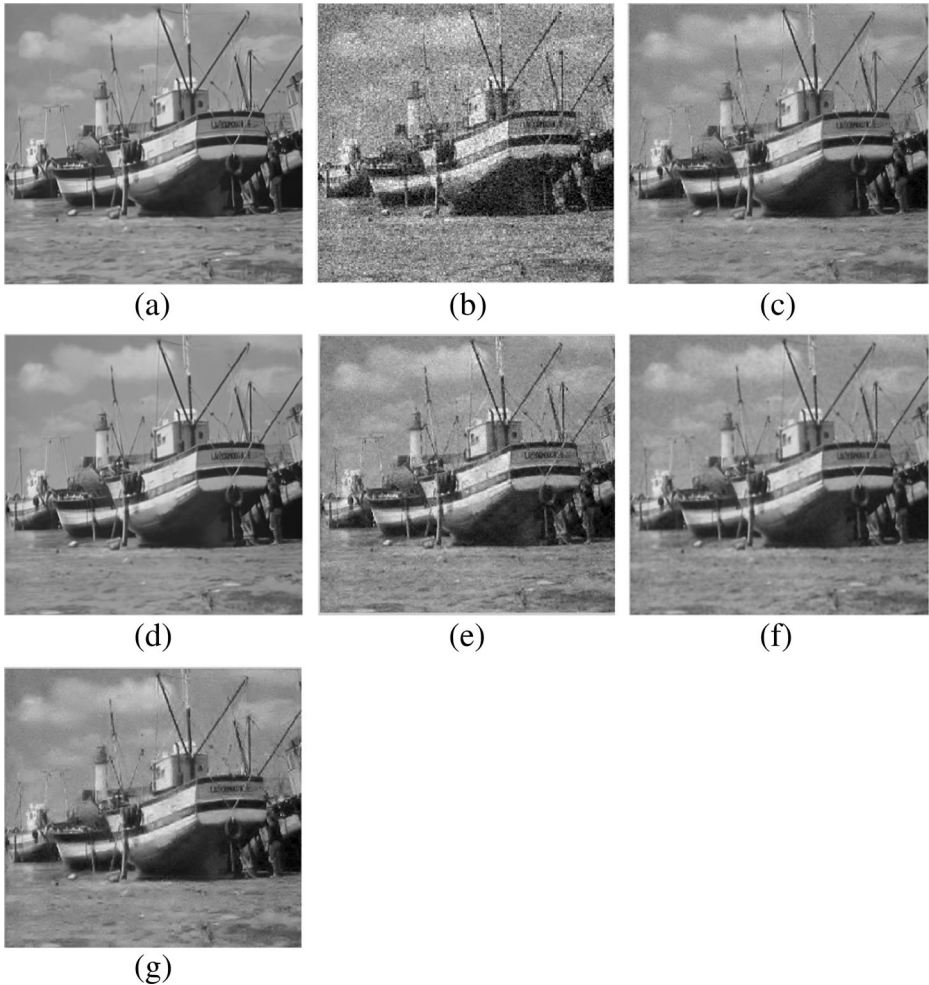


Fig. 6 Comparison of different denoising methods visual results when noise level is 20 for benchmark image Boat. (a) Noise-free image, (b) Noisy image, (c) NLM, (d) Sven et al. [19], (e) Proposed algorithm, (f) Yan et al. [25], (g) Khmag et al. [9]

contaminated image. In the current experiments, all the images have the size of 256×256 . Hence, $K = 3200$ (when $K = 3200$, it consumes a time more than the time as $K = 1600$ consumes) is chosen to give enough candidate choices to every single patch regarding to the variation of appearance results when the K values is changed. The visual effect of the clustering of K-means on one of the benchmark images under testing (Lena) is depicted in Fig. 5. As shown in the figure, the proposed algorithm shows high performance in high frequency component of the tested image, such as the edges, ridges, and fine textures. With comparison to the method in [20], the proposed method very clear distinguishes the grayscale components, which gives more adaptively behavior to the proposed classifications manner (Fig. 4).

4.2 Noise removal quality and assessments

In the practical part the chosen tested benchmark images have been contaminated with AWGN with several noise levels $\sigma = [10, 20, 35, 45, 55, \text{ and } 70]$. Most of recent studies started their noise levels from 10 and above. In addition, in high noise levels many denoising techniques are always prone to have over-smoothing and extra blurring in the crucial image features as well as introducing artifacts. By stating the block label, The PSNR and SSIM several results are shown in Tables 1 and 2. The qualitative findings reveal that the high noise levels yields an image with low visual quality and it causes intensity difference in the patches with the same structures. As can be seen in Fig. 5e, the resulted image which is acquired by the proposed method showed high visual quality especially in Lena hat and hair textures. Additionally, Figs. 6 and 7 shows benchmark images with complicated textures, Boat and Man. The denoised images by the proposed algorithm still kept the fine details such as Boat's mast and Man's hair and cap's feathers textures. Furthermore, Figs. 8 and 9 show benchmark images of Peppers and Straw, both images carry lines curves and complex details. Despite most of state of the art noise

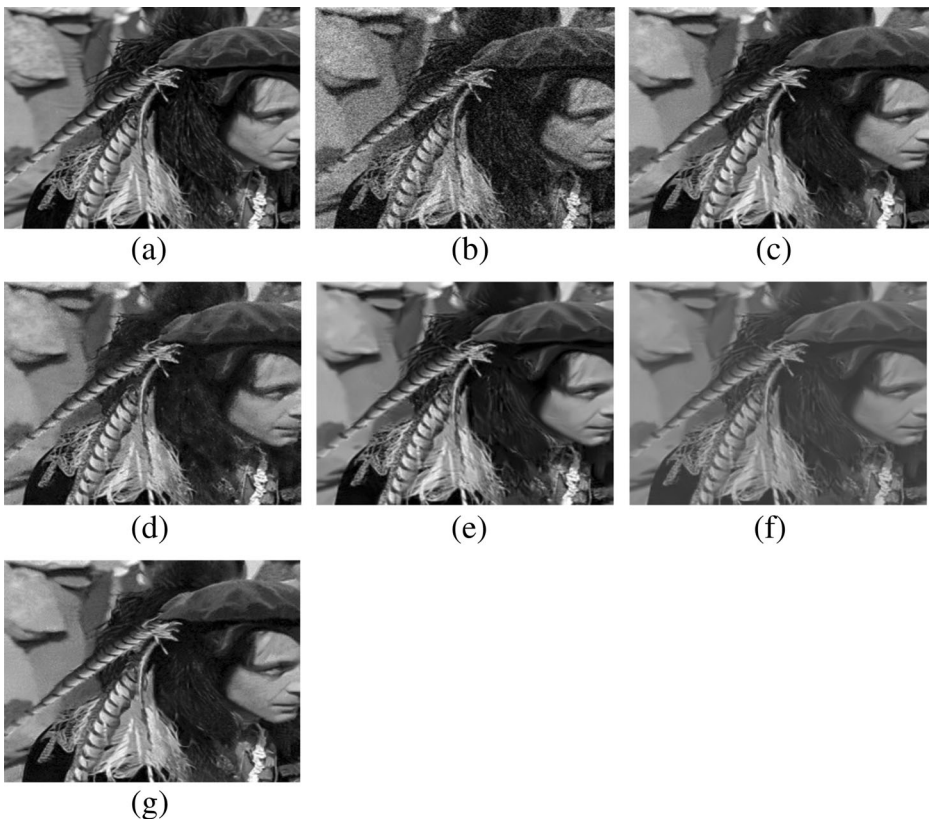


Fig. 7 Comparison of different denoising methods visual results when noise level is 20 for benchmark image Man. (a) Noise-free image, (b) Noisy image, (c) NLM, (d) Sven et al. [19], (e) Proposed algorithm, (f) Yan et al. [25], (g) Khmag et al. [9]

removal methods under investigation failed to keep the core details of the figures as can see in the straw edges and Peppers ridges, the proposed method showed the best performance among the rest techniques. Finally, Fig. 10 shows zoomed in part of Baboon benchmark image. In this figure, the nose and eyes and eyelashes are kept in the proposed technique while most of noise removal methods added some blurring artifacts to their resulted images. Practically, the technique in [25] employs a spatial filter method but is applied to neighborhoods, a practice that may result in a few of correct candidates especially in the case where the variation of the fine details is robust. Therefore, specific patches still contaminated with noise. The proposed technique overcomes this problem by gaining adequate reliable candidates from the clustering of K-means. Figure 8 depicts the subjective results for a benchmark image in the case where the noise level of Gaussian noise is 55. It is worthy to notice that the conventional NLM is mostly ineffective. However, in high noise levels the intensity matching among several patches is very sensitive to noise. The suggested technique adopted wavelet filter as preprocessing step to conquer the additive noise and thus the moment invariants give robustness to

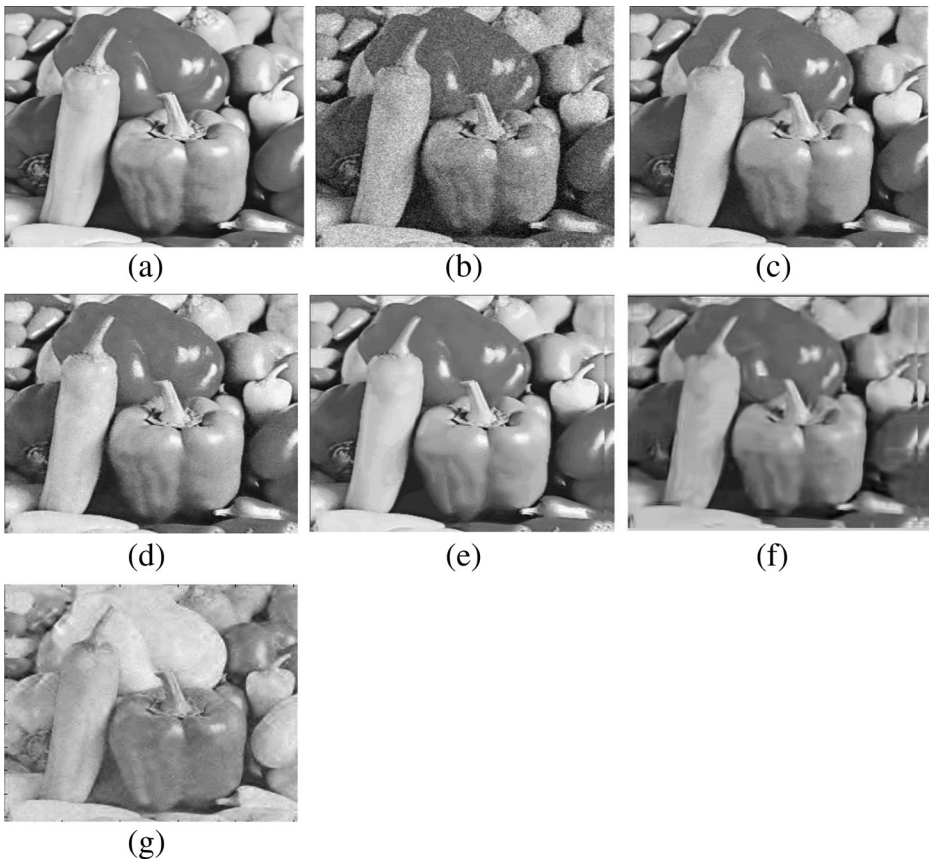


Fig. 8 Comparison of different denoising methods visual results when noise level is 20 for benchmark image Peppers. (a) Noise-free image, (b) Noisy image, (c) NLM, (d) Sven et al. [19], (e) Proposed algorithm, (f) Yan et al. [25], (g) Khmag et al. [9]

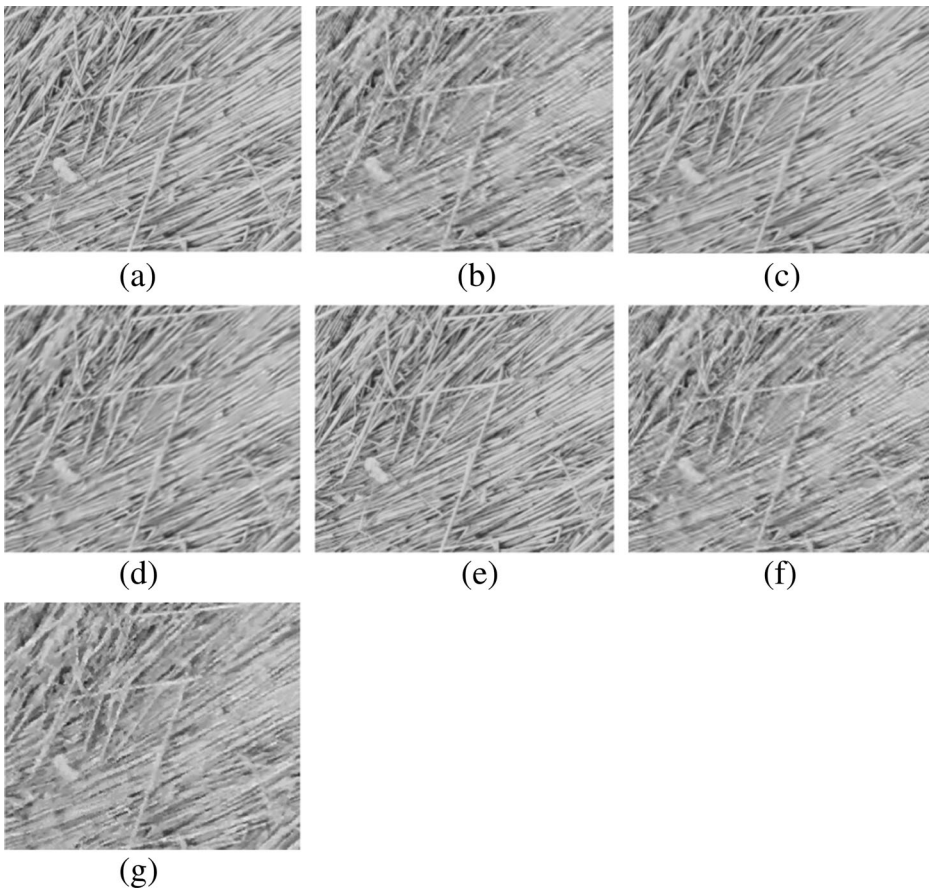


Fig. 9 Comparison of different denoising methods visual results when noise level is 20 for benchmark image Straw. (a) Noise-free image, (b) Noisy image, (c) NLM, (d) Sven et al. [19], (e) Proposed algorithm, (f) Yan et al. [25], (g) Khmag et al. [9]

the proposed algorithm. The method in [19] dealt with rough image configuration but still not enough to keep the fine details of the tested image. The proposed algorithm also preserves the small textures much better in comparison with other methods under investigation. This finding proves that the use of clustering model just before the weighted averaging process can guarantee the reliable candidates and its sub-images. In order to present the execution time of the proposed algorithm and compare it with state of the art noise removal methods, the average run-time of each noise removal method is shown in Table 3. The proposed technique is effectively retaining the main details of the tested image and simultaneously introducing small artifacts in comparison with other techniques. Thus, K-means clustering which is used in the proposed algorithm is a time-consuming method. As future study, it needed to find a clustering approach with fast processing in matching of patch candidates and also to speed up the preclassification process.

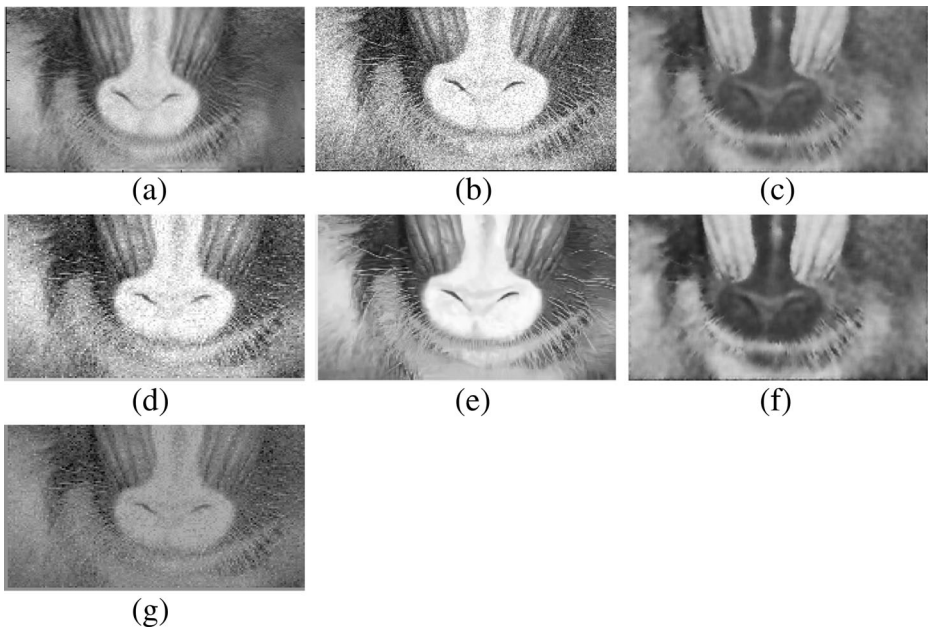


Fig. 10 Comparison of different denoising methods visual results when noise level is 20 for benchmark image Baboon. (a) Noise-free image, (b) Noisy image, (c) NLM, (d) Sven et al. [19], (e) Proposed algorithm, (f) Yan et al. [25], (g) Khmag et al. [9]

5 Conclusion

This study presented a noise removal method that exploited NLM approach in order to suppress the AWGN in natural images. In this regard, moment invariants which represented by K-means clustering and stationary wavelet transformation filtering is used to classify the noisy coefficients from the original and noise free ones. Hidden Markov models is likewise used in order to add some similar sub-images that have been exploited by specific angles to be more strength to the target sub-images and catch the dependencies among similar classes. Experimental results show that moment invariant in the patch clustering has an effective performance in preclassification procedure. The suggested method is successfully retaining the fine details of the investigated image and simultaneously produced small artifacts in comparison with state of the art noise removal techniques. Thus, K-means clustering which is exploited in the proposed algorithm is a time-consuming technique. As future study, it needed

Table 3 Average execution time in Seconds of several noise removal techniques

Image Technique	Man	Monarch	Lena	House	Peppers	Boat	Baboon	F-16	Straw
NLM	5.07	6.02	5.04	4.96	4.84	4.84	4.85	5.13	4.79
Sven et al. [19]	0.61	0.64	0.65	0.65	0.69	0.62	0.64	0.63	0.64
Yan et al. [25]	0.72	0.91	0.58	0.68	1.23	0.74	0.53	0.63	0.79
Khmag et al. [9]	1.22	1.33	1.42	1.34	1.29	1.09	1.31	1.23	1.31
Proposed	1.10	0.94	0.98	1.21	1.11	0.88	0.87	1.22	0.92

to find a clustering method with fast processing in the processing of matching to find out patch candidates as fast as possible to speed up the preclassification step.

References

1. Ahmed F, Das S (2014) Removal of High-Density Salt-and-Pepper Noise in Images With an Iterative Adaptive Fuzzy Filter Using Alpha-Trimmed Mean. *IEEE Trans Fuzzy Syst* 22(5):1352–1358
2. Buades A, Coll B, Morel J-M (2005) A non-local algorithm for image denoising. *IEEE Conf Comput Vis Pattern Recognit* 2:60–65
3. Chen G, Qian S-E (2011) Denoising of hyperspectral imagery using principal component analysis and wavelet shrinkage. *IEEE Trans Geosci Remote Sens* 49(3):973–980
4. Coupé P, Yger P, Prima S, Hellier P, Kervrann C, Barillot C (2008) An optimized blockwise nonlocal means denoising filter for 3-D magnetic resonance images. *IEEE Trans Med Imaging* 27(4):425–441
5. Demir B, Erturk S, Gullu M (2011) Hyperspectral image classification using denoising of intrinsic mode functions. *IEEE Geosci Remote Sens Lett* 8(2):220–224
6. Jafar IF, AlNa'mneh RA, Darabkh KA (2013) Efficient improvements on the BDND filtering algorithm for the removal of high-density impulse noise. *IEEE Trans Image Process* 22(3):1223–1232
7. Khmag A, Ramli R, Al-haddad SAR, Kamarudin NHA, Mohammad OA (2015) Robust Natural Image Denoising in Wavelet Domain using Hidden Markov Models. *Indian J Sci Technol* 8(32):1–9
8. Khmag A, Ramli AR, Al-Haddad SAR, Hashim SJ, Noh ZM, Najih AA (2015) Design of natural image denoising filter based on second-generation wavelet transformation and principle component analysis. *J Med Imaging Health Inform* 5(6):1261–1266
9. Khmag A, Ramli AR, Al-haddad SAR, Yusoff S, Kamarudin NH (2016) Denoising of natural images through robust wavelet thresholding and genetic programming. *Vis Comput* 33(9):1141–1154
10. Khmag A, Ramli AR, Hashim SJ, Al-Haddad SAR (2016) Additive noise reduction in natural images using second-generation wavelet transform hidden Markov models. *IEEJ Trans Electr Electron Eng* 11(3):339–347
11. Khmag A, Ramli AR, Al-haddad SAR, Kamarudin N (2017) Natural image noise level estimation based on local statistics for blind noise reduction. *Soc Comput* 34(2):141–154
12. Li Z, Cheng Y, Tang K, Xu Y, Zhang D (2015) A salt & pepper noise filter based on local and global image information. *Neurocomputing* 159:172–185
13. Lu C-T, Chen Y-Y, Wang L-L, Chang C-F (2016) Removal of salt-and-pepper noise in corrupted image using three-values-weighted approach with variable-size window. *Pattern Recogn Lett* 80(1):188–199
14. Mahmoudi M, Sapiro G (2005) Fast image and video denoising via nonlocal means of similar neighborhoods. *IEEE Signal Process Lett* 12(12):839–842
15. Nayak DR, Dash R, Majhi B (2017) Stationary Wavelet Transform and AdaBoost with SVM Based Pathological Brain Detection in MRI Scanning. *CNS Neurol Disord Drug Targets* 16(2):137–149
16. Roy A, Laskar RH (2016) Multiclass SVM based adaptive filter for removal of high density impulse noise from color images. *Appl Soft Comput* 46:816–826
17. Roy A, Singha J, Manam L, Laskar RH (2017) Combination of adaptive vector median filter and weighted mean filter for removal of high-density impulse noise from color images. *IET Image Process* 11(6):352–361
18. Salmon J (2010) On two parameters for denoising with non-local means. *IEEE Signal Process Lett* 17(3):269–272
19. Sven G, Sebastian Z, Joachim W (2011) Rotationally invariant similarity measures for nonlocal image denoising. *J Vis Commun Image Represent* 22(2):117–130
20. Thaipanich T, Oh BT, Wu PH, Xu D, Kuo CCJ (2010) Improved image denoising with adaptive nonlocal means (ANL-means) algorithm. *IEEE Trans Consum Electron* 56(4):2623–2630
21. Tomasi C, Manduchi R (1998) Bilateral filtering for gray and color images. In: *Sixth IEEE International Conference on Computer Vision, Bombay, India*, pp 839–846
22. Wang Z, Bovik AC, Sheikh HR, Simoncelli E (2004) Image quality assessment: from error visibility to structural similarity. *IEEE Trans Image Process* 13(4):600–612
23. Wang J, Guo Y, Ying Y, Liu Y, Peng Q (2006) Fast non-local algorithm for image denoising. In: *IEEE International Conference on Image Processing*, p 1429–1432
24. Yan R (2014) Adaptive Representations for Image Restoration. PhD Thesis, University of Sheffield, UK
25. Yan R, Shao L, Cvetkovic SD, Klijin J (2012) Improved Nonlocal Means Based on Pre-Classification and Invariant Block Matching. *IEEE/OSA J Disp Technol* 8(4):212–218
26. Zhang P, Li F (2014) A new adaptive weighted mean filter for removing salt-and-pepper noise. *IEEE Signal Process Lett* 21(10):1280–1283

27. Zhang Y, Wang S, Huo Y, Wu L, Liu A (2010) Feature extraction of brain MRI by stationary wavelet transform and its applications. *Int Conf Biomed Eng Comput Sci (ICBECS)* 18:115–132



Asem Khmag was born in Tripoli, Libya. He received the B.Sc. degree from the University of Tripoli, and the M.Sc and the Ph.D. degree in image processing from Universiti Putra Malaysia, Kuala Lumpur, Malaysia, both in computer and communication systems, in 2006 and 2016, respectively. From 2009 to 2012, he was a Lecturer with Zawia University and a Researcher with the Center of Applied Science Research in Zawia city. Dr. Khmag is now Head of computer Systems Engineering in faculty of Engineering. His research interests include image processing, pattern recognition, computer vision and application of computer graphics, cryptography, and security systems. Dr. Khmag is a reviewer of several journals, such as JEST, IAJIT (the International Arab Journal of Information Technology), Journal of Signal, Image and Video Processing springer, Engineering Letters, Entertainment ACM (Association of Computer Machinery), and Walailak Journal of Science and Technology.



Syed Abdul Rahman Al Haddad received the B.Sc. degree in computer science (major: software engineering) from the University Technology, Malaysia, the M.Sc. degree in multimedia engineering from the University Putra Malaysia, Malaysia, and the Ph.D. degree in electrical, electronic and system engineering from the Universiti Kebangsaan Malaysia, Malaysia. Dr. Al-Haddad is a member of the World Academy of Science, Engineering and Technology (WASET), the International Association of Engineers (IAENG), the Malaysia Science Engineering Technology (MSET), and the Malaysia Information Technology Society (MiTS). His research interests include speech processing, office automation, computer telephony, and integrated image processing.



Ridza Azri Ramlee graduated with honors in Electronic Engineering in 2000 and a Master's degree in Telecommunication and Information Engineering in 2008, both from Universiti Teknologi MARA (UiTM), Malaysia. In 2009 he joined the Faculty of Electronics and Computer Engineering, University of Technical Malaysia Melaka (UTeM), Malaysia, where he is currently Senior Lecturer. He has more than 7 years in the engineering industry as an engineer and has a status as a Professional Engineer with Practicing Certificate (PEPC), which was awarded by the board of Engineer Malaysia (BEM) in 2013. He is also active in the IEEE, Institution of Engineers Malaysia (IEM) and Technological Association of Malaysia (TAM). He is now pursuing Ph.D. in Computer Science and Engineering, University Putra Malaysia. His research is on the computer-aided diagnosis of eye diseases (i.e. Corneal Arcus) using image processing. His current research interests include image analysis, classification techniques, statistical learning, and neural networks.



Noraziahtulhidayu Kamarudin received BSc Comp majoring in Software Engineering from Universiti Putra Malaysia, and MSc in Computer Science in Universiti Teknikal Malaysia Melaka. Currently, she is PhD student in the Department of Computer and Communication Engineering, Faculty of Engineering in Universiti Putra Malaysia. Her research interests are in the field of Speech Recognition, Identification and signal processing, Quranic Audio Processing, Noise and Echo Cancellation, Mobile Location Based Services and Mobile Speech Recognition.



Fahad Layth Malallah USM / Malaysia, also, coordinator & Computer Science, Cihan University / Iraq,. He has graduated since 2008 and 2014 for Bsc (Mosul University / computer Engineering). And MSc (UPM / Computer Engineering) respectively. He also has worked for 3 - year with an international telecommunications such as Huawei, Nokia and Siemens with specialist in Intelligent Network (IN-GSM) Senior Engineer. In terms of academic scientific research, he has a contribution around the world as he has published many article papers with reputed inte as many international conferences. He is dedicating his time for Computer Vision, Image Processing and Information Security researching. His native tongue is Arabic with fluent in English language, basic in both French and Kurdish Languages.